An Energy-Based Harmonic Constitutive Law for Magnetic Cores With Hysteresis

Martin Hafner, François Henrotte, Mercedes Herranz Gracia, and Kay Hameyer

Institute of Electrical Machines, RWTH Aachen University, D-52062 Aachen, Germany

In this paper, a phenomenological energy-based material model for ferromagnetic materials under harmonic conditions is presented. The model is based on the concept of a complex effective permeability and an accurate representation of energy is adopted as identification criteria. The material model is implemented in a time-harmonic finite element model, which allows to solve for the loss characteristics of electromagnetic devices. Identification is based on measured hysteresis loops and no additional fitting parameters are required. Hysteresis losses in a ferromagnetic C-core and a ferromagnetic torus are simulated and compared to the results obtained by means of tabulated loss characteristics.

Index Terms—**Energy storage, finite-element methods, harmonic analysis, magnetic hysteresis, magnetic losses.**

I. Introduction

In (standard) FEA iron loss analysis, hysteresis losses are determined together with eddy current losses by means of measured loss curves. As standard loss measurement gives total losses in function of applied field and frequency, it is not surprising that a subsequent separation of both nonlinear loss effects is difficult. Nevertheless, the evaluated iron losses comply with the experiment.

However, when the question of hysteresis losses arises, the accuracy of total losses is no longer sufficient. An energy-based constitutive material law for the finite element analysis is required that provides a material model (hysteresis) on the one hand, and a physical, phenomenological loss tracking (depending strongly on the magnetic behavior) on the other. The derived material representation is implemented in the time-harmonic finite element analysis. This allows computing simultaneously the flux distribution (based on the effective reluctivity concept) and hysteresis losses.

The hysteresis characteristics for this material law is provided by the energy-based vector hysteresis model proposed in [1]. Comparable results would be obtained with any other model providing a real (ferromagnetic) material curve with a true interpretation in terms of energy.

II. Theoretical Setup

A. General Frequency Domain Approaches

The time-harmonic material law assumes a linear relation between the magnetic field H [A/m] and the flux density B [T]. The amplitude and the phase relation of the quantities H and B may vary, but both are of the same frequency

$$\underline{\mathbf{H}} = \underline{\nu} \cdot \underline{\mathbf{B}}. \tag{1}$$

According to the following general correlation of an arbitrary function $\mathbf{f}$ in the time and the frequency domain:

$$\mathbf{f} = \Re\{\mathbf{F}e^{j\omega t}\} \quad \partial_t \mathbf{f} = \Re\{j\omega \mathbf{F} e^{j\omega t}\} \tag{2}$$

the complex reluctivity $\underline{\nu} = \nu_r + j\nu_i$ of (1) is represented as the time domain operator ν

$$\nu = \nu_r + \frac{\nu_i}{\omega}\partial_t. \tag{3}$$

If now time characteristics $\mathbf{h}(t)$ and $\mathbf{b}(t)$ in a material with saturation and dissipation are considered, one can write the equality

$$\mathbf{h}(t) = \nu \mathbf{b}(t) + \Delta\mathbf{h}(t) \tag{4}$$

where ν is the linear operator (3), which corresponds to the complex reluctivity in the frequency domain, and $\Delta\mathbf{h}(t)$ is the representation error, i.e., the error due to the representation of the material law by a complex reluctivity.

Using (4), the conservation of energy states

$$\mathbf{h} \cdot \partial_t \mathbf{b} = \nu_r \partial_t |\mathbf{b}|^2 + \frac{\nu_i}{\omega}|\partial_t \mathbf{b}|^2 + \Delta\mathbf{h} \cdot \partial_t \mathbf{b} \tag{5}$$

where $\nu_r \partial_t |\mathbf{b}|^2$ is the change of the magnetic stored energy. The positive term $\frac{\nu_i}{\omega}|\partial_t \mathbf{b}|^2$ represents the rate of the dissipated energy.

Thanks to this relation (5), one can give an interpretation in terms of energy of the error induced by choosing different complex reluctivities $\underline{\nu} = \nu_r + j\nu_i$ to represent the nonlinear dissipative material law.

Different choices are indeed possible that lead to holding the error term $\Delta\mathbf{h}$ equal to zero in some sense.

1) Orthogonality in space: choosing ν so as to have $\Delta\mathbf{h}(t) \perp \partial_t \mathbf{b}(t)$, where $\Delta\mathbf{h}$ and $\mathbf{b}$ are of the same frequency, is artificial and, therefore, not further considered.
2) Orthogonality in the frequency domain: ν_r is chosen so that $\nu_r \mathbf{b}$ corresponds to the fundamental harmonic of $\mathbf{h}(t)$. Then, one has

$$\int_0^T \Delta\mathbf{h} \cdot \partial_t \mathbf{b} dt = 0 \tag{6}$$

because $\Delta\mathbf{h}$ contains only higher harmonics which means that the energy balance of the material is correctly represented.

This approach ensures a correct representation of the stored magnetic energy and of the dissipated energy over one pe-

Digital Object Identifier 10.1109/TMAG.2007.916141

Color versions of one or more of the figures in this paper are available online at http://ieeexplore.ieee.org.

riod in the material. However, on the other hand, the magnetic field $\mathbf{h}(t)$, with all higher harmonics cutoff, is poorly represented and considerably underestimated.

3) A third approach consists in defining $\nu_r = \nu_{\min}$ such that

$$\max_{\mathrm{T}} |\mathbf{h}(t)| = \nu_{\min} \max_{\mathrm{T}} |\mathbf{b}(t)| \Rightarrow \Delta\mathbf{h} = 0, \qquad \dot{\mathbf{h}} = 0. \tag{7}$$

This approach ensures that the amplitude of the magnetic field is correctly represented but it overestimates significantly the stored energy.

4) Orthogonality over one period: the fourth approach consists in defining $\nu_r = \nu_{\mathrm{ave}}$ such that

$$\nu_{\mathrm{ave}} \int_0^T \mathbf{h}(t) \cdot \mathbf{b}(t) dt = \int_0^T \mathbf{h}^2(t) dt \tag{8}$$

which means that

$$\int_0^T \Delta\mathbf{h} \cdot \mathbf{h} dt = 0 \tag{9}$$

the representation error is orthogonal to the field, or in other words, the positive and negative errors cancel out over one period.

This approach, which is the classical definition of the effective permeability in the literature [2], ensures a good representation of the reluctivity in average over one period. It is the approach used in this paper (cf. Fig. 1).

B. Harmonic Constitutive Law

The reluctivity given in (8), called "effective reluctivity" ν_{ave} in literature, is considered to be a good approximation for time-harmonic finite element computations, as described in [3] and [4]. Assuming (1) can be written in terms of phasors (8), one has

$$|\underline{\nu}|\ |\underline{\mathbf{B}}| \equiv \nu_{\mathrm{ave}}\, \mathbf{b} \tag{10}$$

which leads to a constraint for the magnitude of the complex reluctivity

$$|\underline{\nu}| = \frac{\int_0^T \mathbf{h}^2(t) dt}{\int_0^T \mathbf{h}(t) \cdot \mathbf{b}(t) dt}. \tag{11}$$

The imaginary part of the complex reluctivity represents the hysteresis losses in the material.

Assuming now that $\Delta\mathbf{h} = 0$, one has by integrating (5) over one period that the dissipated energy

$$w_\mu = \int_0^T \mathbf{h}(t) \cdot \partial_t \mathbf{b}(t) dt \tag{12}$$

$$= \int_0^T \frac{\nu_i}{\omega} |\partial_t \mathbf{b}(t)|^2 dt \tag{13}$$

$$= T\omega\nu_i |\underline{\mathrm{B}}|^2 \tag{14}$$

from where the identification follows:

$$\nu_i = \frac{\int_0^T \mathbf{h}(t) \cdot \partial_t \mathbf{b}(t) dt}{T\omega |\underline{\mathrm{B}}|^2}. \tag{15}$$

According to (15), the energy dissipation w_μ in time depends on the imaginary part ν_i of the complex reluctivity $\underline{\nu}$. The definition of $|\underline{\nu}|$, and therefore, ν_r relies on the concept of effective permeability which minimizes the periodic average energy error. In case of the time-harmonic constitutive law, defined by (11) and (14), the magnetic field strength $\mathbf{h}$ and the flux density $\mathbf{b}$ comply simultaneously with a measured magnetization loop.

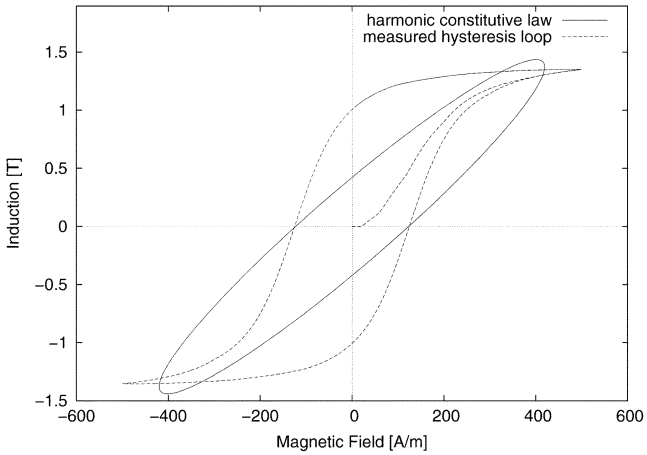

Fig. 1. Comparison of a hysteresis loop and the flux density $\mathbf{B}$ obtained with the time-harmonic law for an uniaxial magnetic field strength $\mathbf{H}$ with an amplitude of 500 A/m.

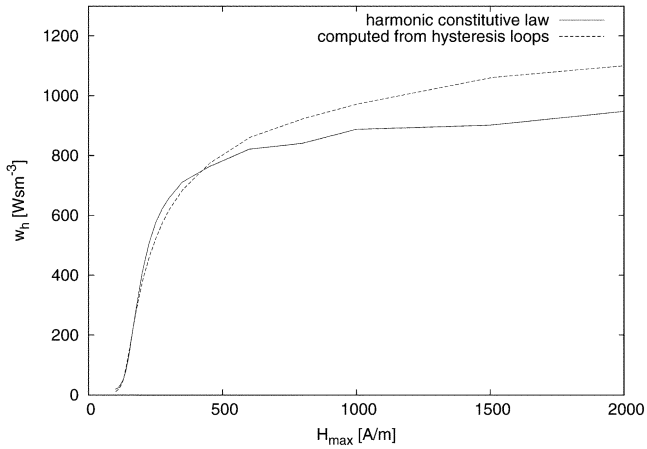

Fig. 2. Specific hysteresis losses $\mathrm{w_h}$ in function of the applied magnetic field strength $\mathrm{H_{max}}$.

Fig. 1 compares a measured hysteresis loop for an uniaxial magnetic field strength $\mathbf{H}$ with an amplitude of 500 A/m to the flux density $\mathbf{B}$ obtained by the previously defined harmonic constitutive law. As a matter of frequency analysis, the variation of $\mathbf{H}$ and $\mathbf{B}$ in time is elliptical. Its area is equal to the hysteresis loop area. Furthermore, the figure exhibits, as known from the literature, a slight overestimation of the material induction.

III. Implementation

Equations (11) and (14) state an energy-based time-harmonic constitutive law. The derived complex reluctivity $\underline{\nu}$ constitutes a true correlation of the flux density $\mathbf{B}$ to the magnetic field $\mathbf{H}$ in terms of mean energy and is applicable to the governing equation of the time-harmonic (3-D) problems

$$\mathrm{curl}\ (\underline{\nu}\ \mathrm{curl}\ \underline{\mathbf{A}}) = \underline{\mathbf{J}_s} \tag{16}$$

where $\underline{\mathbf{A}}$ is the magnetic vector potential and $\underline{\mathbf{J}_s}$ is the applied current source density.

In order to solve (16) by means of the finite element method, one basically has to update the value of the reluctivity $\underline{\nu}$ as a function of the 3-D flux density solution $\mathbf{B} = \mathrm{curl}\mathbf{A}$ after each calculational step. The algebraic system of complex equations can be solved iteratively to fulfill the steady-state condition. This method is called successive substitution. A direct adaptation of

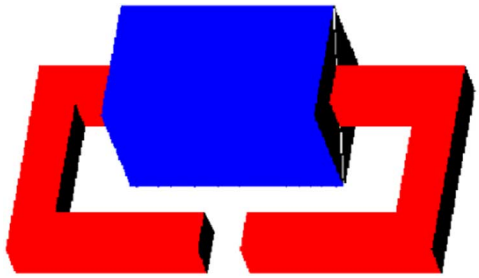

Fig. 3. C-core as the test model for the hysteresis loss calculation.

the Newton–Raphson method is not possible, because the derived energy-based reluctivity is complex and not monotone.

The $\nu - \mathbf{B}$ function is implemented as a map that associates the characteristic parameters ν_r and ν_i to every possible variation of the flux density distribution $\mathbf{B}$. The entries of this preliminary calculated lookup table that have been calculated in a previous step are provided by the energy-based vector hysteresis model [1].

The sketched numerical solving process is realized by modifying the $\mathbf{A}$-approach of Harm3D, a frequency-domain solver of the iMoose solver environment [5] for solving (16) in the linear case.

IV. Validation Concept

In the time-harmonic case, the hysteresis model parameters are directly based on a set of measured hysteresis loops [1]; its energy balance (stored magnetic energy, dissipated energy) consequently relies on this data.

The necessary hysteresis data B(H) has been identified by a toroid with two coils. One coil had been used to create a time-varying magnetic field H in the cross section of the samples shape. The second coil measured the resulting magnetic flux density response B.

In order to validate the described approach, the loss results, obtained from the energy-based time-harmonic calculation, are compared to postprocess loss estimation routines of the time-domain finite element simulation. Due to this, all required characteristics, magnetic reluctivity as well as hysteresis loss curves, are derived from the same measured hysteresis data to minimize the differences between both numerical approaches.

In case of the postprocess loss estimation the points of the hysteresis loss density curves $\mathrm{w_h}$ are computed by

$$\left.\begin{matrix}\mathrm{w_h(B\ max)}\\ \mathrm{w_h(B_{1,peak})}\end{matrix}\right\} = \oint_c \mathrm{H}\cdot d\mathrm{B} \tag{17}$$

in function of the maximal measured flux density $\mathrm{B_{max}}$ and the peak value of the fundamental induction $\mathrm{B_{1,peak}}$, where H and B are the measuring points of a hysteresis loop. Fig. 2 shows, independent from the chosen estimation value $\mathrm{B_{max}}$ or $\mathrm{B_{1,peak}}$, the computed hysteresis loss density in function of the applied magnetic field strength H.

V. Results

A. Study-Case C-Core

A C-core, sketched in Fig. 3, with a steel volume of 0.002 $\mathrm{m^3}$, is used as a test model for the loss estimation approaches described in Section IV. The source current density J_s is injected into the cross-section area of the coil. The surrounding of the C-core as well as the aperture are modeled as air.

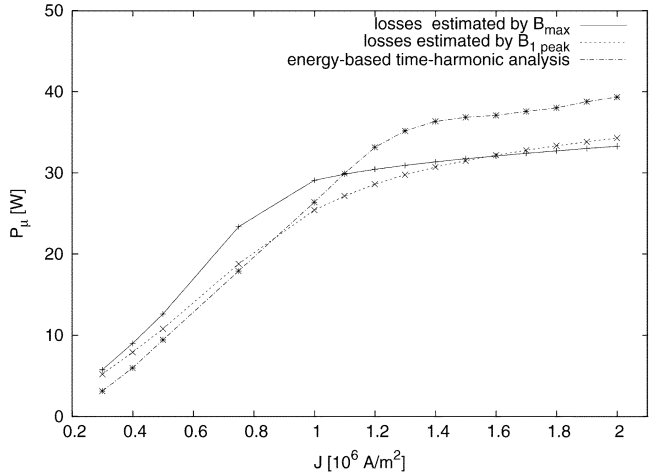

Fig. 4. Hysteresis losses P_μ in function of the effective coil current density J_s for the transient and time-harmonic approaches.

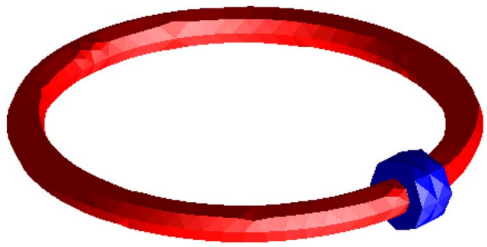

Fig. 5. Torus as the test model for the hysteresis loss calculation.

Fig. 4 shows the hysteresis losses P_μ in function of the effective coil current density J_s obtained by the time-domain postprocessing loss estimations evaluating $\mathrm{B_{1,peak}}$ and $\mathrm{B_{max}}$, and the modified frequency-domain computation. For the unsaturated case ($J_s \leq 10^6$ A/m), the losses calculated by the harmonic constitutive law are basically located closely to both transient estimation routines; the results may be considered to be in expectable agreement. For higher current densities $J_s > 1.0 \cdot 10^6$ A/m, a saturation effect can be noticed in all hysteresis loss approaches; a saturation phenomena is observed and all loss curves converge to a common maximal value. As expected, both transient estimations are of the same shape and merge for current densities $J_s \rightarrow 2 \cdot 10^6$ A/m. In saturation, transient and time-harmonic loss estimations deviate by about 10%.

B. Study-Case Torus

A torus, sketched in Fig. 5, with a steel volume of $8.67 \cdot 10^{-5}$ $\mathrm{m^3}$, is used as a second test model for the described loss estimation approaches. This electromagnetic test device is directly excited by a current I that flows in the modeled coil. The surrounding of the torus is modeled as air, but in contrast to the C-core model there is no air gap in the flux path. Therefore, the magnetic resistance only depends on the steel reluctivity which generally makes a magnetic analysis very sensitive with respect to the variations of the excitation.

Fig. 6 shows the hysteresis losses P_μ in function of the amplitude of the coil current I obtained by the time-domain post processing loss estimations evaluating $\mathrm{B_{1,peak}}$ and $\mathrm{B_{max}}$, and the

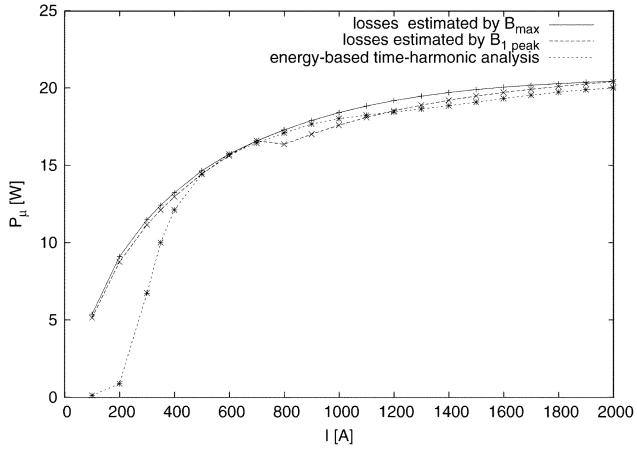

Fig. 6. Hysteresis losses P_μ in function of the amplitude of coil current I for the transient and time-harmonic approaches.

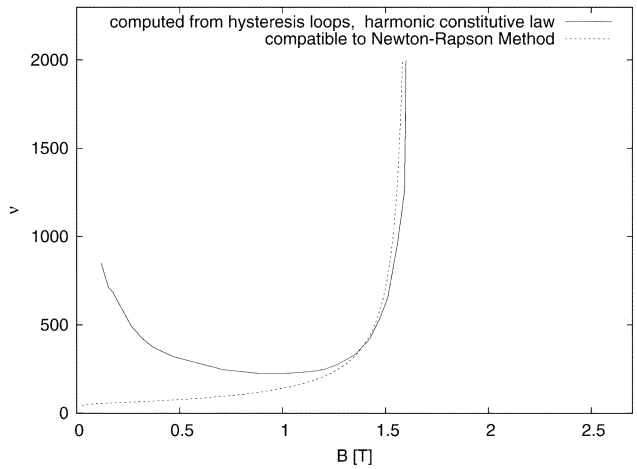

Fig. 7. Comparison between the Newton–Rapson compatible and the measured initial magnetization curves.

modified frequency-domain computation. For coil currents $I \geq$ 500 A, all hysteresis loss curves are in excellent agreement. For coil currents $I \leq 500$ A, both postprocessed loss curves describe a smooth arc ending in the point of origin, whereas the loss curve of the energy-based time-harmonic analysis drops rapidly. The latter loss curve reaches loss values near zero for the excitation below 200 A.

For a coil current below 500 A, the transient and time-harmonic loss estimations start to differ and diverge more and more for decreasing values of I. The reason for this paradoxical behavior is the completely different modeling of the magnetization curve in the lower range of the magnetic field strength H. The magnitude of the complex reluctivity, based on the energy-based hysteresis model, describes the magnetization as a "bathtub" curve which increases for low values of the magnetic field strength H; this curve progression is in agreement with the measured magnetization curves. The magnetization curve of transient 3-D finite element solver has to comply with the requirements of the Newton–Rhapson method. These requirements are satisfied by a monotonically increasing approximation function of the magnetization curve which prohibits a realistic modeling of the reluctivity in the lower range of H; in that range, the reluctivity is near constant (compare Fig. 7).

The equivalent magnetic circuit diagram described by the analytic equation of Ampere's law is defined as $\Phi = R_m \cdot \Theta$, where Θ is the magnetic flux, R_m is the magnetic resistance, and Φ is the magnetomotive force. The coil current I is proportional to the magnetic field strength H. The shape of the hysteresis loss curve, computed by the measured hysteresis loops (cf. Fig. 2), is identical to the loss curve of the modified time-harmonic analysis.

This strongly indicates that, in case of the torus model, the time-harmonic hysteresis loss estimation is more realistic than the estimation of both transient loss routines.

VI. Conclusion

Periodic phenomena are ubiquitous in electromagnetic applications but, due to the magnetic saturation or the presence of nonlinear electronic components, actual wave shapes are scarcely sinusoidal, which invalidates the phasor representation. Still, the complex formalism and the associated time-harmonic analysis are so practical that it is worth to seek the approximative phasor representations for early design stages of new devices. In that case, it is meaningful to adopt the energy as the identification criteria for the definition of equivalent nonlinear material characteristics for these time-harmonic models. The presented approach extends the concept of effective reluctivity by an energy-based hysteresis loss calculation during the traditional solving process. The described method does not require additional fitting parameters, because the hysteresis loss values are based on an energy-based vector hysteresis model [1], which interprets the physical and phenomenological field quantities in terms of the energy.

For both considered case studies, the total hysteresis losses obtained by the constitutive material law are in fair agreement with loss values obtained by measured loss curves. In present state, the applied time-harmonic governing equation does not consider the eddy current term. Taking eddy currents into account, further investigations are necessary to clarify weather improvements on the energy-based time-harmonic constitutive law and its finite element implementation are needed.

References

[1] F. Henrotte, A. Nicolet, and K. Hameyer, "An energy-based vector hysteresis model for ferromagnetic materials," *Int. J. Comput. Math. Electr. Electron. Eng.*, vol. 25, no. 1, pp. 71–80, 2006.

[2] S. J. Salon, *Finite Element Analysis of Electrical Machines*. New York: Kluwer, 1998.

[3] E. Vassent, G. Meunier, and J. Sabonnadiere, "Simulation of induction machine operation using complex magnetodynamic finite elements," *IEEE Trans. Magn.*, vol. 25, no. 4, pp. 3064–3066, Jul. 1989.

[4] G. Arians, *Numerische Berechnung Der Elektromagnetischen Feldverteilung, Der Strukturdynamischen Eigenschaften und Der Geräusche der Asynchronmaschine*. Berlin, Germany: Shaker Verlag.

[5] G. Arians, T. Bauer, C. Kaehler, W. Mai, C. Monzel, D. van Riesen, and C. Schlensok, "Innovative modern object-oriented solving environment—iMOOSE," 2007 [Online]. Available: http://www.imoose.de

Manuscript received June 24, 2007. Corresponding author: M. Hafner (e-mail: Martin.Hafner@IEM.RWTH-Aachen.de).